

RESEARCH

Open Access



# Experimental Investigation on Seismic Resistance of RC Shear Walls with CFRP Bars in Boundary Elements

Jun Zhao<sup>1</sup>, Fuqiang Shen<sup>2,3\*</sup> , Chenzhe Si<sup>1</sup>, Yuping Sun<sup>3</sup> and Lu Yin<sup>2</sup>

## Abstract

Experimental investigation on seismic performance of RC shear walls reinforced with CFRP bars in boundary elements to enhance the resilience was presented which is expected for stable resistance capacity and small residual deformation. Six RC shear walls reinforced with CFRP bars as longitudinal tensile materials in boundary elements were tested under reversed cyclic lateral loading while subjected to constant axial compression with different axial load ratios of 0.17, 0.26 and 0.33, respectively. Two forms of stirrups were used for each axial load ratio, which were rectangular and circular stirrups in boundary elements. A reference specimen, ordinary RC shear walls, was also introduced to certify the excellence of CFRP bars. The test results indicated that the walls utilizing CFRP bars had small residual deformations and residual crack widths. Lower crack propagation height and larger concrete crushing region, bearing capacity and equivalent viscous damping coefficient (EVDC) could be observed with the increase of axial load ratios. The effects of stirrup forms on experimental results had a relation to the axial load ratio. When the axial load ratio was small, the shear walls with circular stirrups had better energy dissipation than that with rectangular stirrups at a given drift level, while the cumulative energy dissipation (CED) were similar. With the increase of axial load ratio, the walls exhibited similar energy dissipation at the same drift level, however, the shear walls with rectangular stirrups had larger CED.

**Keywords:** shear wall, CFRP bar, seismic performance, residual deformation, axial load ratio, stirrup form

## 1 Introduction

In recent years, the earthquakes have caused serious damages because of higher magnitude and longer lasting time than before, the increasing quantities of earthquakes occurred beyond the seismic fortification intensities in the earthquake-prone regions (Li et al. 2008; Chen and Zheng 2016). Besides, the aftershocks after the main earthquakes became more and more frequently. According to the current seismic design codes in most countries, it was acceptable that the structures have severe

damages as long as no collapse happened after the moderate and strong earthquakes. These structures could result in huge threats to lives and properties in the following aftershocks or reoccurring earthquakes without collapse in the main earthquake. In 2009, the earthquake resilient structure was proposed to balance the serious damages by earthquakes and the security of structures. Earthquake resilient structures referred to the structures that could recover serviceability with simple repairs and maintenance in some conditions or even need not to be repaired after moderate and strong earthquakes (Lu et al. 2014; Jiang and Liu 2015; Lu et al. 2017).

Shear walls were widely used to enhance the earthquake resistance of middle- and high-rise building structures because of the excellent seismic performance. However, with the development of earthquake-resistant

\*Correspondence: shenfq\_edu@163.com

<sup>2</sup> School of Civil Engineering, Zhengzhou University, Zhengzhou, Henan 450001, China

Full list of author information is available at the end of the article

design philosophy, the conventional shear walls cannot meet the requirements of resilient structures. As a result, many new-type shear walls were proposed to cope with the serious earthquake disasters. Experiments on prestressed concrete shear walls were conducted and proved that prestressed reinforcements could provide resilience and reduce the residual deformation effectively (Dang et al. 2013, 2014; Wu et al. 2016). Yuan et al. (2018) proposed a kind of concrete walls reinforced by PC strands to obtain significant drift-hardening capability up to 2.5% with reduced residual deformation and crack width. Besides, High performance concrete can also be employed to improve the performance of shear walls. Tong et al. (2016) found that the reactive powder concrete could improve crack pattern and bearing capacity in his experimental study on reactive powder concrete shear walls (Tong 2016, Tong and Fang 2016). Steel-plate composite shear walls were also researched by many scholars in recent years. These walls have good deformation capacity and ductility (Takahashi et al. 1973; Clublely et al. 2003a, b; Eom et al. 2009). The seismic performance could also be improved by setting apertures in the walls (Hitaka and Matsui 2003; Tong et al. 2005). In summary, new materials and structures could optimize the seismic behavior of conventional shear walls to adapt to the new demands of earthquake fortification.

Fiber reinforced composite (FRP) bar is a new-type of composite building material with the excellent characteristics of corrosion resistance, high tensile strength and linear-elastic stress–strain relationship. FRP bars can be utilized as the reinforcing bars in concrete structures in lieu of general steel bars (Du et al. 2012; Gao et al. 2001; Bi 2013). Brown and Bartholomew (1993) investigated FRP bars reinforce concrete beams experimentally. The results revealed that the beams had ideal performance. Cai et al. (2017) placed carbon fiber reinforced composite (CFRP) bars with steel bars in concrete columns and conducted quasi-static tests, then found that CFRP bars could enhance the stiffness of columns after yielding and reduce the residual deformation up to over 2.4% drift. In the tests on columns reinforced with CFRP bars under reversed cyclic lateral loading, Gong et al. (2010) found that concrete columns reinforced with CFRP bars had higher bearing capacity and deformation capacity, the axial load ratio and volume percentage of stirrup were the predominant influence factors on the seismic performance of columns. Hasaballa et al. (2011) conducted tests on beam-column joints reinforced with glass fiber reinforced composite (GFRP) bars and stirrups under simulated seismic loading and found that these joints sustained up to 3.0% drift safely without considerable damage. Besides, many other researches also demonstrated that FRP bars could replace steel bars entirely or partly in conventional concrete

structures to perfect the performance of these structures (EI-Gamal et al. 2005; Tobbi et al. 2012; EI-Mogy et al. 2013).

Placing the GFRP bars having high strength and linear elasticity can improve the performance of shear walls. Ghazizadeh and Cruz-Noguez (2018) conducted experimental and analytical study on low-rise RC walls reinforced with GFRP bars and steel fibers, of which results showed that utilizing GFRP bars could make walls achieve well seismic performance with less residual displacements. The study of Mohamed et al. (Mohamed 2013; 2014a, b) on shear walls reinforced with GFRP bars also illustrated that the residual deformation of shear walls reinforced with GFRP bars were obviously smaller than that of ordinary shear walls. Besides, the shear wall reinforced with GFRP bars with little residual deformation had good resilience when the load was less than 80% of the ultimate load. In conclusion, GFRP bars can effectively reduce the residual deformation of shear walls and benefit the resilience of shear walls.

The research team of the authors have studied the shear walls reinforced with CFRP bars and found that placing CFRP bars in the proper position could enhance the bearing capacity and reduce the residual deformation (Chen 2015; Zhao 2016; Zeng 2017).

Based on the above researches, this paper investigates the effects of the axial load ratio and stirrup form in boundary elements on shear walls reinforced with steel bars and CFRP bars as the longitudinal reinforcing bars in boundary elements.

## 2 Experimental Program

### 2.1 Details of Specimens

Six identical geometry specimens with the same reinforcement details but different forms of stirrups in boundary elements were fabricated and tested. Figure 1 shows the dimensions and reinforcement details of the specimens. The boundary elements of specimens CFRPRW had rectangular stirrups and of the specimens CFRPHW had circular stirrups in boundary elements. Both rectangular and circular stirrups in boundary elements were 6 mm-diameter HPB300 steel bars with spacing of 50 mm. Eight 12 mm-diameter CFRP bars and four 8 mm-diameter steel bars were placed in each boundary element as longitudinal bars. Vertical and horizontal web reinforcement for all specimens were HRB335 steel bars with the diameter of 8 mm. The vertical web reinforcement consisted of two layers of steel bars spaced at 60 mm, and the horizontal web reinforcement also consisted of two layers of steel bars, while the spacing of which were 50 mm and 70 mm, respectively, in the region below the height of 600 mm from the base and the upper region. The high-strength and non-contrast

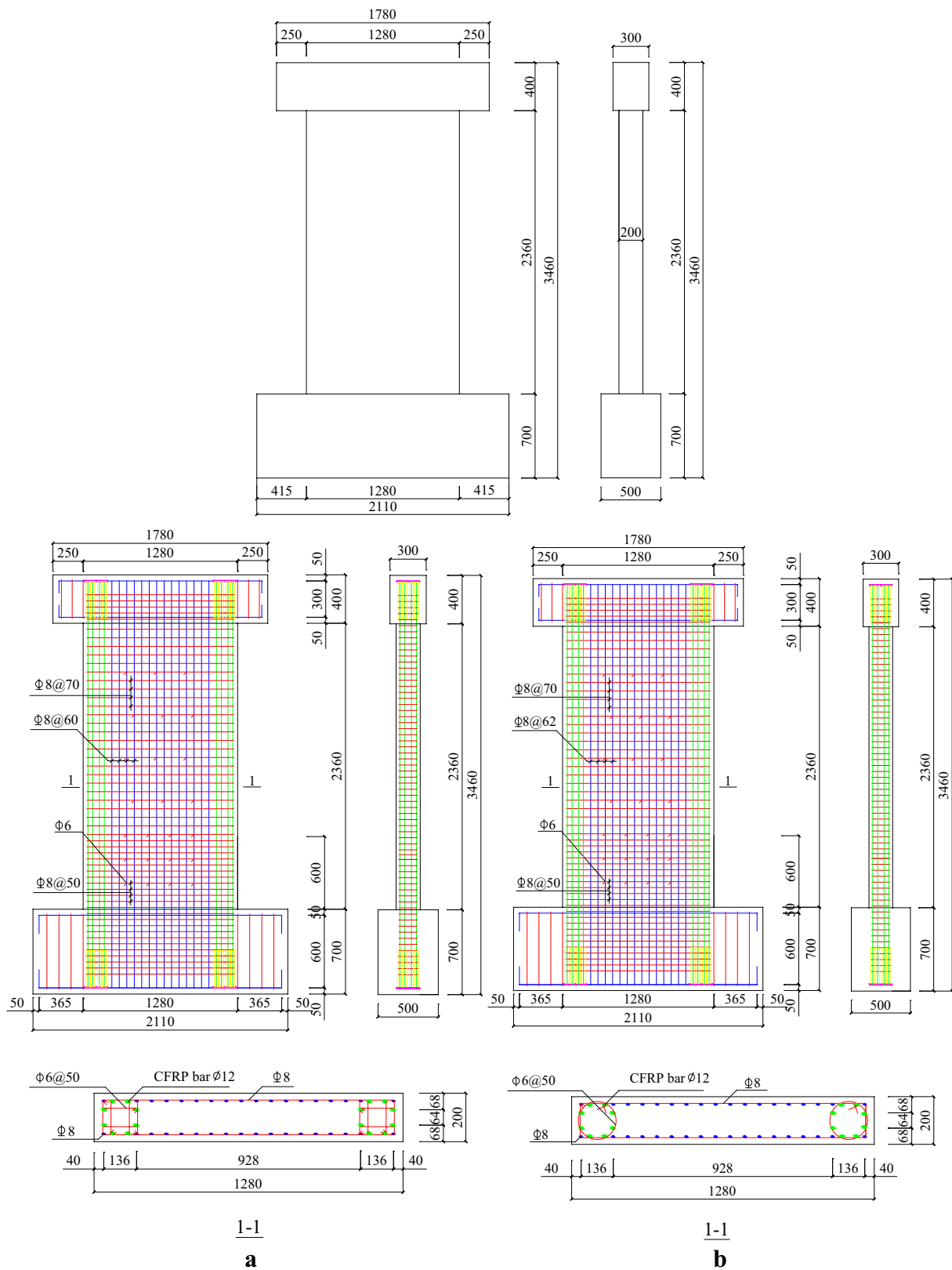


**Fig. 1** Schematic representation and reinforcement of specimen (**a** CFRPRW, **b** CFRPHW).

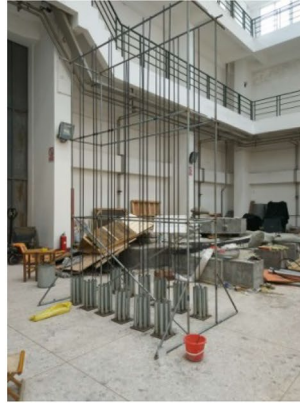


**Fig. 2** Anchorage setup for CFRP bar.

**Table 1** Properties of bars.

Bars	Diameter/mm	Yield strength/MPa	Ultimate strength/MPa	Yield strain/ $\mu\epsilon$	Elongation/%	Modulus/MPa
HPB300	6	414.8	529.4	1860	19.4	$2.23 \times 10^5$
HRB335	8	361.3	502.6	1599	19.2	$2.26 \times 10^5$
CFRP bar	12	–	2310.3	–	–	$1.43 \times 10^5$

grouting material were used between the end of CFRP bars and sleeves welded on steel plate to enhance the bond between CFRP bars and concrete for the purpose of avoiding slip and ensuring the maximum performance of CFRP bars as shown in Fig. 2.

The axial load ratios of the specimens were 0.17, 0.26 and 0.33, respectively. CFRPRW1 and CFRPHW1 were tested under quasi-static reversed cyclic loading with the axial load ratio of 0.17. CFRPRW2 and CFRPHW2 were tested with the axial load ratio of 0.26. CFRPRW3 and CFRPHW3 were tested with the axial load ratio of 0.33.

Besides the six concrete shear walls reinforced with CFRP bars mentioned above, a reference specimen, RCSW, which was RC shear walls reinforced with deformed steel bars in boundary elements, was also tested under the axial load ratio of 0.17. RCSW had the same geometry and longitudinal reinforcing bars and stirrups except the longitudinal reinforcements in boundary elements compared with CFRPRW1. Besides, RCSW was tested with the test methods which was the same as CFRPRW1. The experimental program of RCSW was introduced in detail in another literature of the author (Zhao 2019).

**2.2 Material Properties**

Ready-mixed concrete was used to cast the specimens, and the concrete cubic (150 mm length) strength,  $f_{cu}$ , was 57.2 MPa. The concrete prismatic (300 mm high by



**Fig. 3** Loading setup.

150 mm length) strength,  $f_c$ , was 36.8 MPa. The mechanical properties of CFRP bars and steel bars are shown in Table 1.

**2.3 Test Methods**

The test apparatus is shown in Fig. 3. The foundation beam of shear wall was anchored to the laboratory floor and restrained by four hydraulic jacks and two steel beams to eliminate horizontal slip and vertical movement. Cyclic lateral loading was applied through the MTS servo-controlled hydraulic actuator at a height of

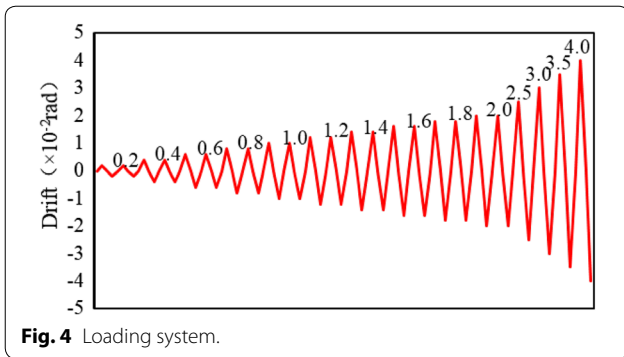


**Fig. 4** Loading system.

2560 mm from the top surface of the foundation beam. A constant axial compressive load was applied by two hydraulic jacks on the top of the loading beam. And a sliding mechanism was installed between the vertical hydraulic jacks and reaction beam to ensure that the hydraulic jack can move with the specimen, leading to constant vertical loading.

Reversed cyclic lateral loading was controlled by the drift ratio, which was the ratio obtained by dividing the lateral top displacement by the shear span. The loading program was shown in Fig. 4. Two cycles were applied at each drift level with increments of 0.2% up to 2.0%. In subsequent loading, one cycle was applied at the drift levels of 2.5%, 3.0% and 3.5%, respectively.

Measuring and recording of the strains of reinforcement and concrete, as well as the displacements of

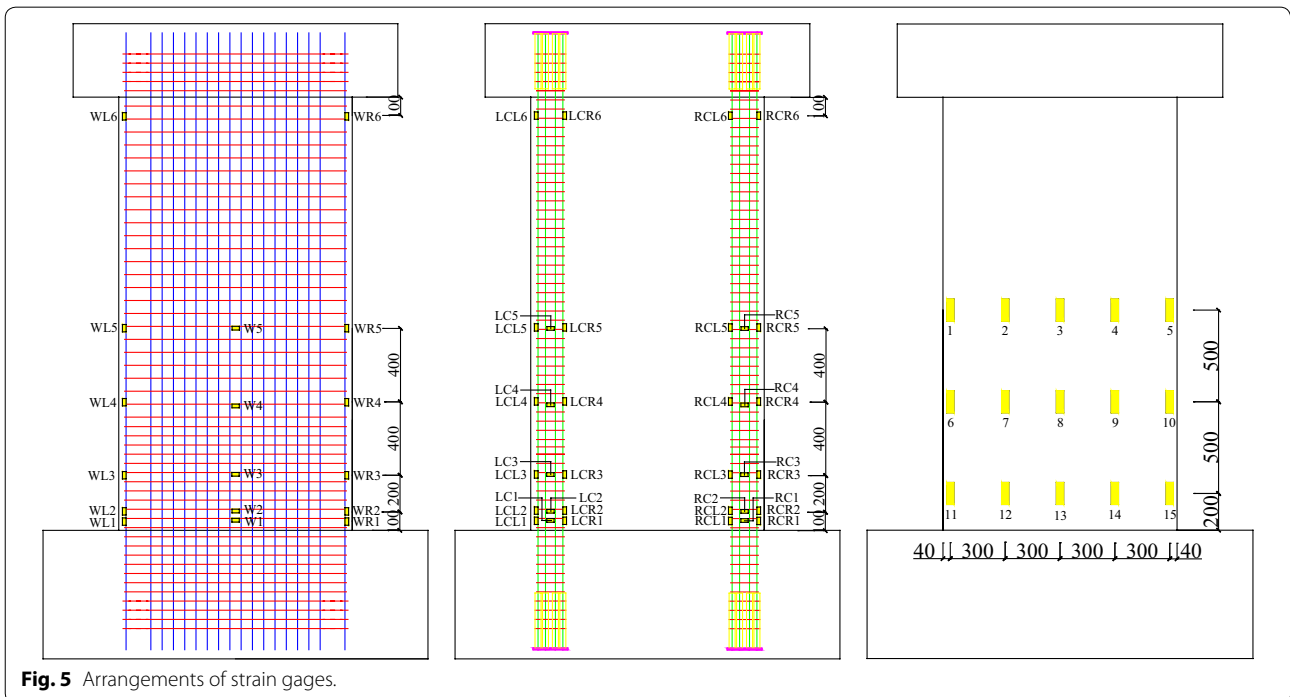
specimens were carried out in the test. The strains of reinforcement and concrete were measured by strain gages with the locations as shown in Fig. 5. Strain gages were placed on CFRP bars, steel bars in the wall panel, and stirrups in the boundary elements. Figure 6 showed the locations of displacement transducers to measure the displacements of different heights of shear walls.

### 3 Experimental Results

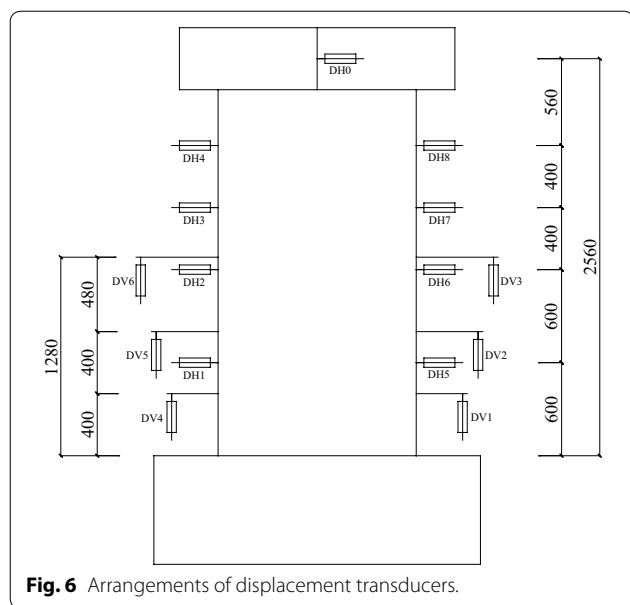
#### 3.1 Crack Pattern and Failure Mode

Figure 7a, b show the crack patterns and failure modes of RCSW and CFRPRW1, respectively. Both of them experienced a flexure-shear failure mode. The cracks propagated more adequately on the façade of CFRPRW1 compared with that of RCSW. The reason account for that phenomenon was that the CFRP bar was a kind of linear-elastic material with high tensile strength and low bond strength. Then there was no too large plastic deformation on CFRP bars at hinge region. Besides, the low bond strength allowed CFRP bars to slip in concrete. So cracks distributed along the whole height of CFRPRW1. It can also be observed that concrete spalling of RCSW was more serious than that of CFRPRW1. The conclusion can be drawn that placing CFRP bars in boundary elements can improve crack propagation and concrete spalling.

The crack patterns and failure modes of CFRPRW1 and CFRPHW1 were shown in Fig. 7b, c, respectively. CFRPRW1 presented the typical flexible-shear failure



**Fig. 5** Arrangements of strain gages.



**Fig. 6** Arrangements of displacement transducers.

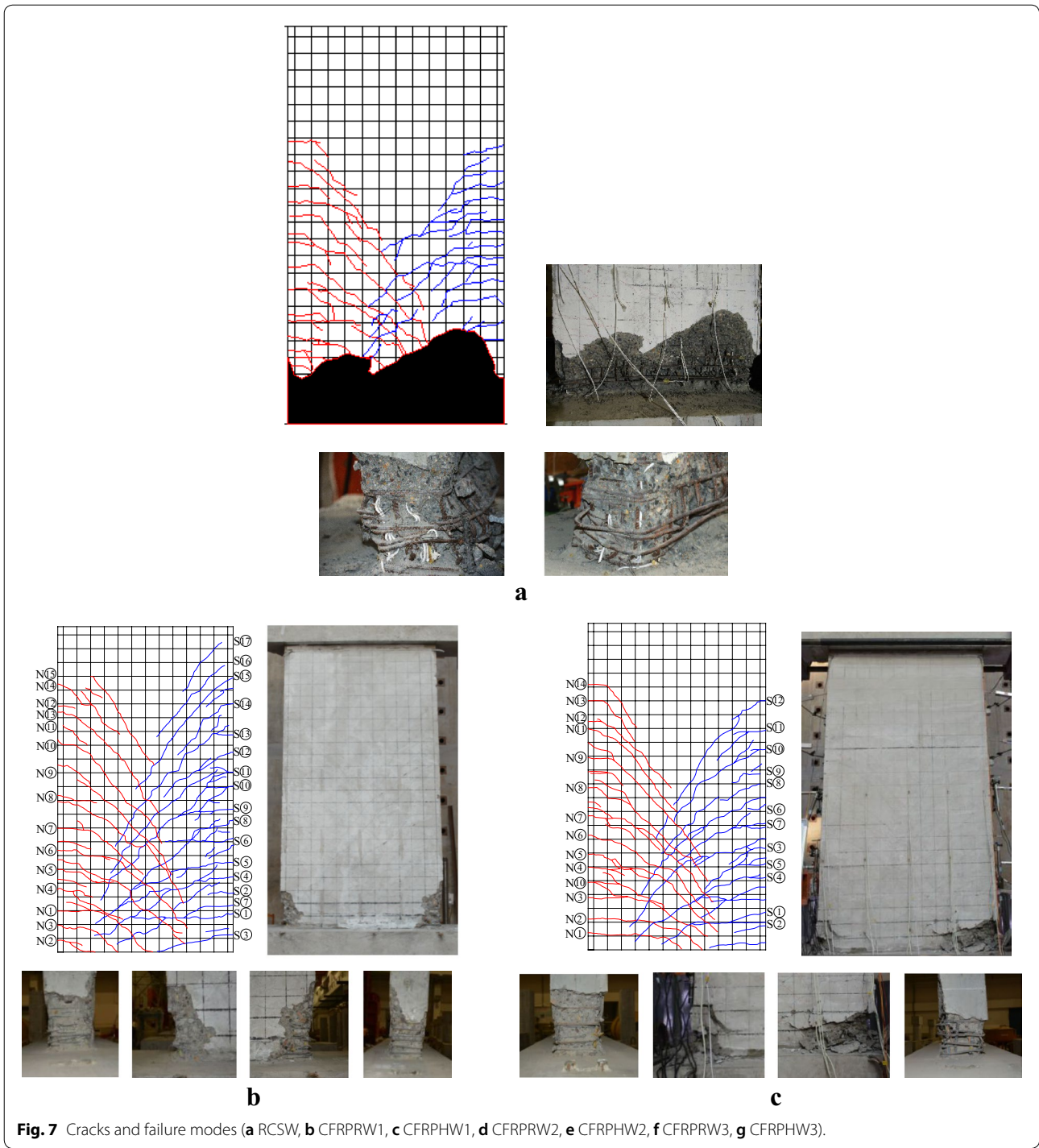
mode. The first horizontal crack was observed near the bottom corner of the wall at the drift ratio of 0.4%, while the diagonal crack appeared after the 0.6% lateral drift, and meanwhile the yielding of outermost longitudinal steel bars occurred. As loading continued, the cover concrete near the wall toe began to spall when drift ratio reached 1.6%. And with the displacement increased, the load reached the peak value at the lateral drift of 2.5%, followed by the ultimate drift ratio of 3.0%. As shown in Fig. 7b, cracks sufficiently propagated with the distribution of the whole height of the wall panel and the spacing of approximately 100 mm. The concrete spalling region with 300 mm in height and 200 mm in depth could be observed. CFRPHW1 had the similar crack pattern and failure mode with CFRPRW1. At the lateral drift of 0.2%, a horizontal crack initiated before the 0.4% drift at which the first horizontal crack on CFRPRW1 was observed. As the lateral load increased, the diagonal crack and yielding of steel bars were observed at the same drift ratio of 0.6% with CFRPRW1, while the spalling of concrete cover at the 1.2% drift was earlier than that of CFRPRW1. The peak load and ultimate lateral drift of CFRPHW1 were of 2.5% and 3.0%, respectively, which were the same with CFRPRW1. And as shown in Fig. 7c, the height of crack propagation, the height and depth of concrete cover spalling were 1900 mm, 200 mm and 250 mm, respectively. Then it could be concluded that there were no noticeable differences in crack pattern and failure mode between CFRPRW1 and CFRPHW1.

CFRPRW2 and CFRPHW2 were tested under the 0.26 axial load ratio. The first horizontal crack appeared on

the bottom section of CFRPRW2 at the drift of 0.4%. When the drift ratio reached 0.6%, the diagonal crack was observed and the outermost longitudinal steel bars yielded. The concrete spalling emerged at the drift ratio of 1.4%. Then the load increased to the peak value as the drift went to 1.8%, after which the load began to drop down and was terminated after the cycle of 3.0%. Cracks distributed through the height up to 1700 mm of the wall panel. Concrete spalling mainly occurred in the bottom area of wall panel with 250 mm height and 400 mm depth as shown in Fig. 7d. The crack pattern and failure mode of CFRPHW2 were shown in Fig. 7e. The horizontal crack and diagonal crack emerged at the lateral drift of 0.2% and 0.6%, respectively. As the lateral displacement increased, the cover concrete began to spall at the drift ratio of 1.4%. After that, CFRPHW2 reached peak load at 1.8% drift, then the load began to decline and was terminated after the cycle of 2.5%. Cracks propagated along the height of the wall panel and distributed within 1600 mm height. The concrete spalling occurred in the bottom area with 250 mm height and 550 mm depth.

CFRPRW3 and CFRPHW3 were tested under vertical load of the 0.33 axial load ratio. CFRPRW3 cracked horizontally at the 0.4% drift ratio. With the drift ratio increased to 0.6%, diagonally crack and the yielding of longitudinal steel bars appeared. Then the cover concrete began to spall when the drift ratio reached 1.4%. With the increase of displacement, CFRPRW3 reached the peak load at the 1.6% drift ratio, then the load began to decline and was terminated after the cycle of 2.5%. Cracks were distributed up to the height of 1600 mm of the wall panel as shown in Fig. 7f. The height and depth of spalling cover concrete were approximately 210 mm and 400 mm, respectively. As for the specimen of CFRPHW3, the first horizontal crack was observed at the lateral drift of 0.2%. Then the wall panel began to crack diagonally when the drift ratio reached to 0.6% and meanwhile the longitudinal steel bars yielded. The cover concrete spall at the drift ratio of 1.2%. After that, the load reached peak value at the 1.6% drift, then began to decline and was terminated after the cycle of 2.5%. Crack propagation distributed through the 1700 mm height of wall panel. The concrete spalled with the height of 300 mm and the depth of 450 mm as shown in Fig. 7g.

As suggested above, the axial load ratio has relatively significant effects on the failure modes and crack patterns of specimens. When the axial load ratio increased, the crack propagation was restrained, the height of crack reduced and the concrete cover spalling became serious. While shear walls had the similar failure progression and crack propagation at the same axial load ratio, which indicates that the form of stirrup had little influence on these experimental responses at the same axial load ratio.



### 3.2 Hysteretic Curves

The hysteretic curve illustrating the lateral load–displacement response is usually used to analyze the seismic performance of shear wall since it presents structure strength, stiffness degradation and energy

dissipation under cyclic loading effectively. Figure 8 shows the hysteretic curves of specimens.

The hysteretic curve of RCSW exhibited typical ductile characteristics. The lateral force reached the maximum

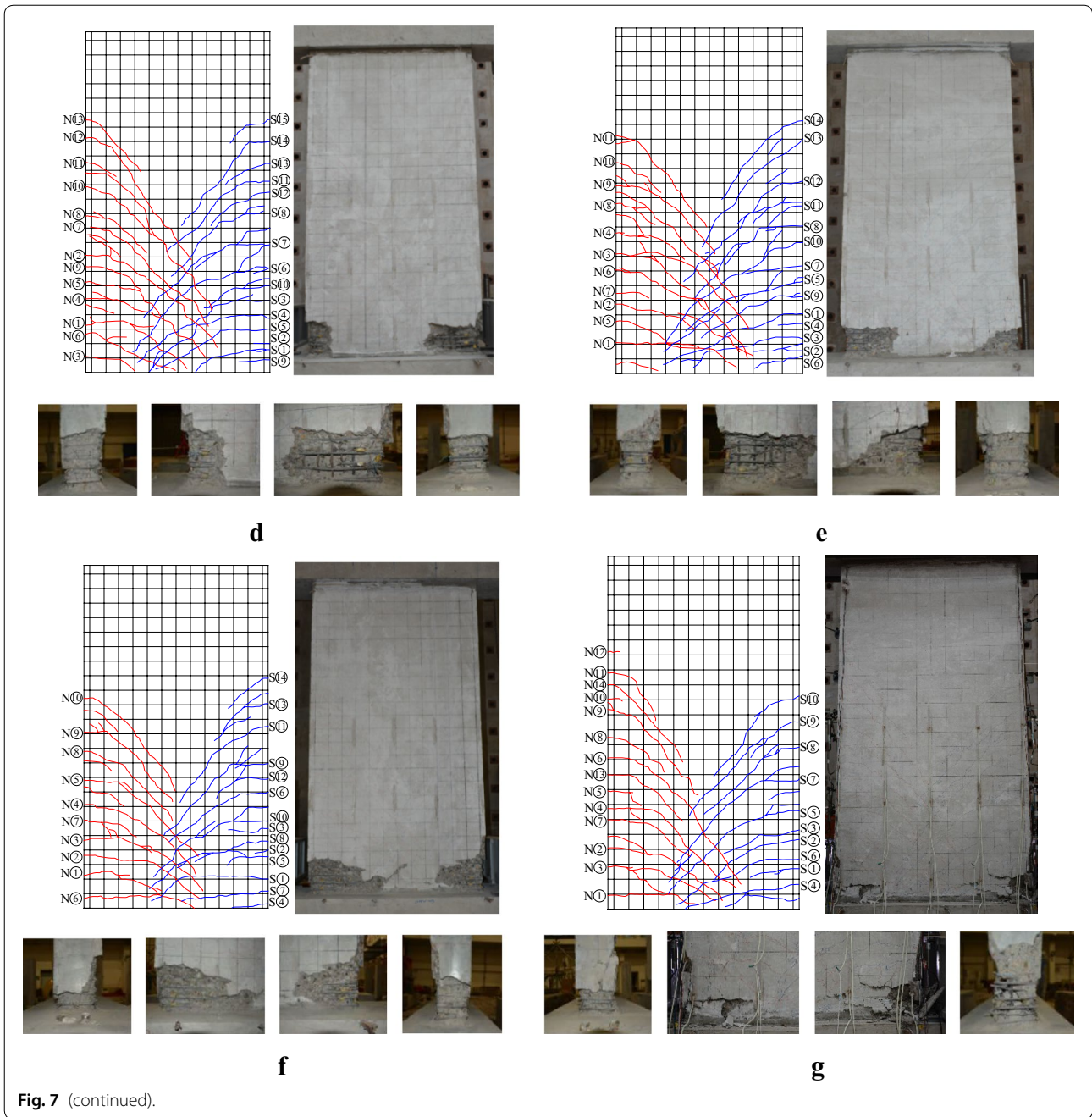
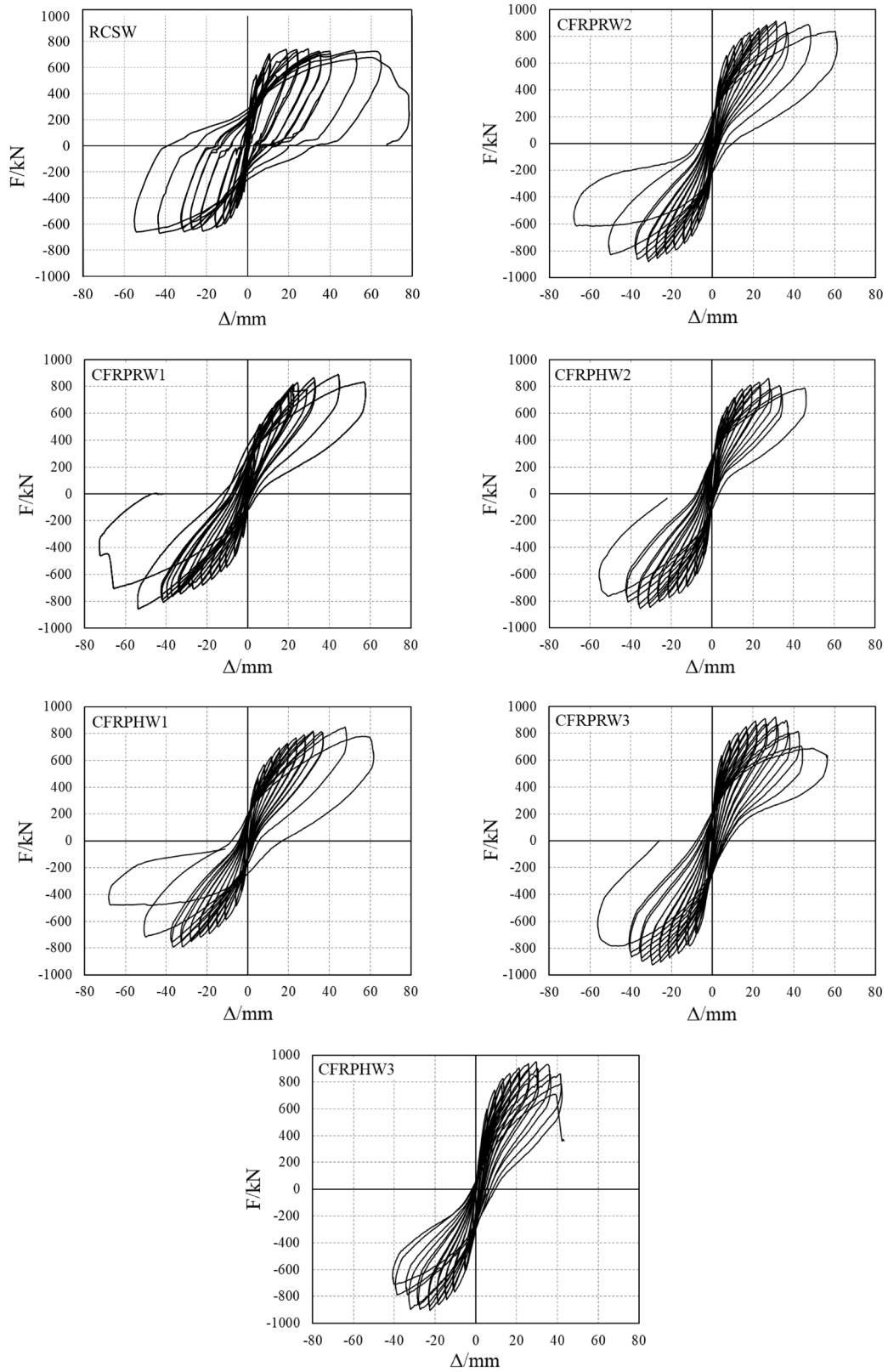


Fig. 7 (continued).

value at small displacement level and then didn't rise with large residual deformation until failure.

In general, the hysteresis loops of walls reinforced with CFRP bars were on rising stage and the load increased with the augment of deformation up to peak load. For shear walls with the axial load ratios of 0.17 and 0.26, there were a slightly decline after the load reached the maximum value, which revealed that shear walls exhibited

stable cyclical behavior up to large deformation without any apparent deterioration of capacity. However, when the axial compression ratio increased to 0.33, an obvious decline of capacity occurred after the maximum value, and the rate of capacity degradation became faster along with the increase of lateral deformation. At the unloading stages, all hysteresis curves approached toward the force axis, which indicated that all shear walls had little residual



**Fig. 8** Hysteretic curves.

deformations after unloading, especially when the drift was less than 1.5%, the residual deformation reached almost 0.

CFRP bars in boundary elements could enhance the lateral resistance as well as reduce the residual deformation, which satisfy well with the requirements, stable resistance and little residual deformation of resilient structures.

### 3.3 Skeleton Curves

Figure 9 presents the skeleton curves of the specimens under different axial load ratios of 0.17, 0.26 and 0.33. The ultimate displacement and the corresponding load were plotted on the curves. According to Fig. 9a, CFRPRW1 had the peak load of 888.77 kN which was 20.1% larger than that of RCSW with the similar ultimate displacement. As for shear walls using CFRP bars, the peak load increased with the increasing axial load ratio, while the displacement at the peak load and the ultimate displacement showed the opposite tendency. At the axial load ratios of 0.17 and 0.26, the skeleton curves almost maintained the stable trend with slight decline. While the skeleton curves of specimens at the axial load ratio of 0.33 presented obvious decline branch, which was more obvious for CFRPRW3 with rectangular stirrups than CFRPHW3 with circular stirrups. Figure 9b showed the comparison of specimens with rectangular stirrups at different axial load ratios. Taking CFRPRW1 as the reference, the peak loads of CFRPRW2 and CFRPRW3 increased by 2.9% and 2.7%, respectively. And CFRPRW2 experienced the similar ultimate displacement with CFRPRW1, however, that of CFRPRW3 was 26.14% smaller. As for the specimens having circular stirrups, the peak loads of CFRPHW2 and CFRPHW3 increased by 4.7% and 8.1%, and the ultimate displacements decreased by 21.14% and 28.15% respectively compared with CFRPHW1.

The skeleton curves of the specimens with different forms of stirrups and axial load ratios were compared in Fig. 9d–f. At the axial load ratios of 0.17 and 0.26, CFRPRW1 and CFRPRW2 reached higher peak loads than CFRPHW1 and CFRPHW2. While as the axial load ratio increased to 0.33, the peak load of CFRPRW3 was similar with CFRPHW3. As for the ultimate displacement, when the axial load ratio was 0.17, CFRPRW1 and CFRPHW1 exhibited the almost same ultimate displacement indicating that the form of stirrup had no significant influence on that at this axial load ratio. As the axial load ratio reached 0.26, the ultimate displacement of CFRPRW2 with rectangular stirrups was 30.90% larger than CFRPHW2 with circular stirrups. While the ultimate displacements of the pair of specimens were similar at the 0.33 axial load ratio.

## 4 Analyses and Discussions

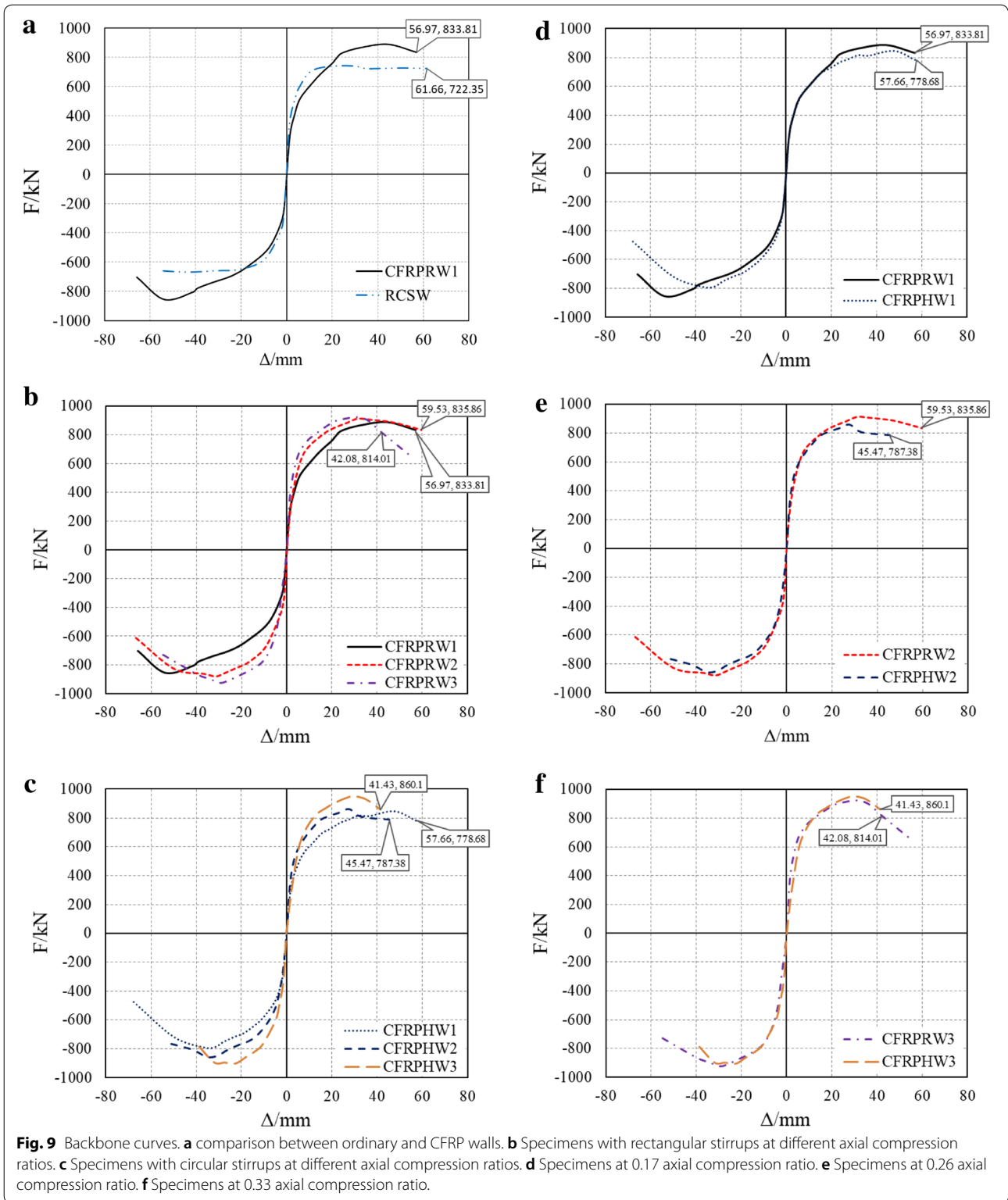
### 4.1 Energy Dissipation

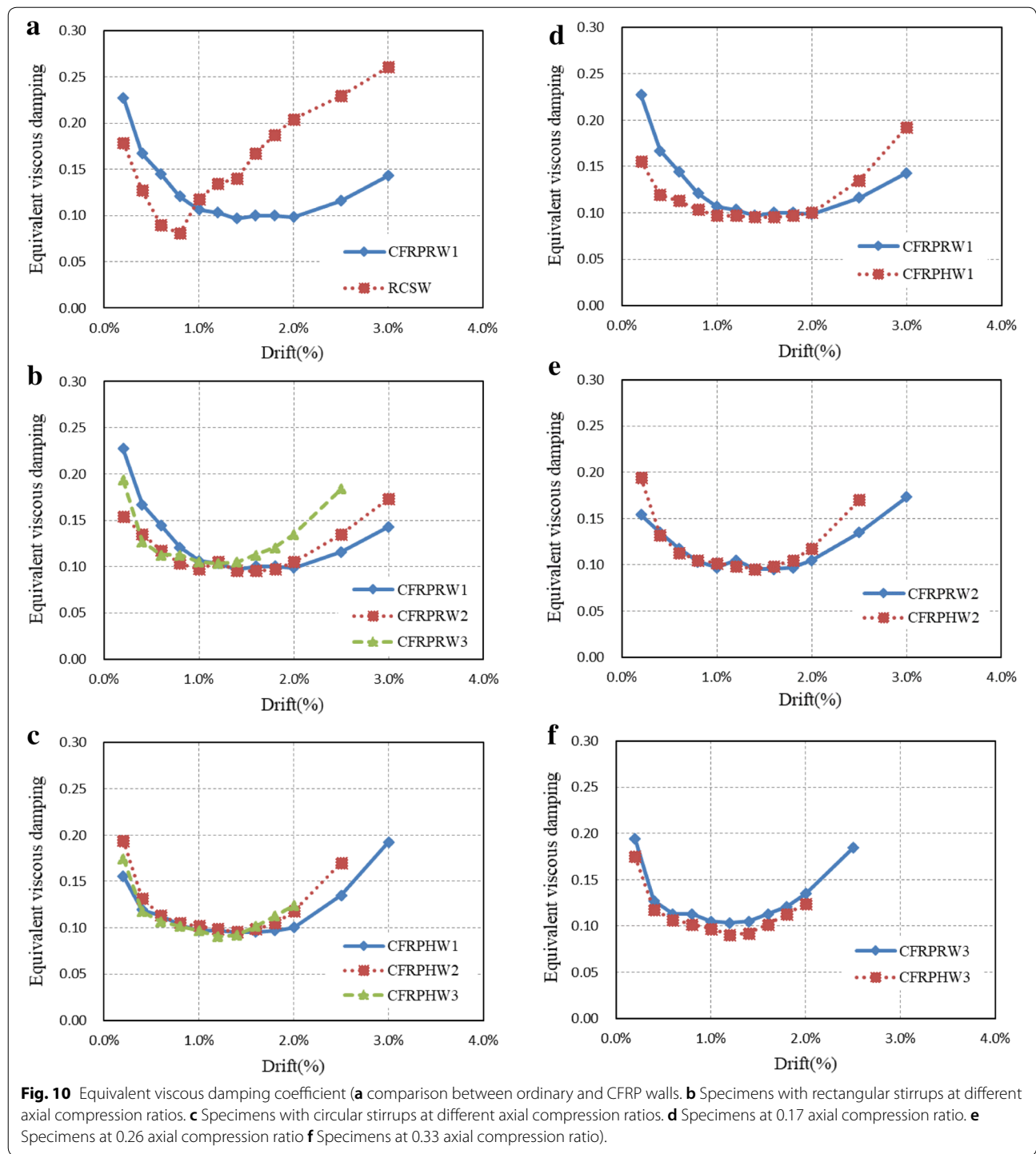
The energy dissipation capacity of the shear walls was evaluated using the equivalent viscous damping coefficient (EVDC) and cumulative energy dissipation (CED) based on the Chinese Specification for Seismic Test of Buildings (2015). Figure 10a shows the EVDC-drift relationships of RCSW and CFRPRW1. RCSW had larger EVDC compared with CFRPRW1 because of the plastic deformation of deformed steel bars. Then the conclusion that ordinary RC shear walls had well energy dissipation capacity than CFRP reinforcing walls can be drawn. As one can see in Fig. 10b, c, EVDC of the shear walls reinforced with CFRP bars at different axial load ratios are compared. There was an inverted triangle trend of the EVDC-drift relation curve. In general, EVDC reached the minimum value at 1.4% drift and then increased to the maximum value until failure. And EVDC was in positive correlation with the axial load ratio at a given drift. Figure 10d–f compared EVDC of the shear walls with two kinds of stirrups. It can be observed that EVDC decreased and then increased at the axial load ratios of 0.17 and 0.26, and EVDC of the shear walls using circular stirrups were larger than those of the specimens using rectangular stirrups at relatively large lateral deformation level. While the shear walls with different stirrups had the approximate same EVDC at the axial load ratio of 0.33.

The CED of shear walls were shown in Table 2. On one hand, the influences of the axial load ratio on CED were related to the form of stirrup. For shear walls with rectangular stirrups, the CED of CFRPRW2, which was similar with CFRPRW3, increased by 23.86% compared with that of CFRPRW1. As for specimens confined by circular stirrups, no noticeable difference of CED among CFRPHW1, CFRPHW2 and CFRPHW3 could be observed. On the other hand, the influences of the form of stirrup on CED also concerned with the axial load ratio. When the axial load ratio was 0.17, the form of stirrup had little effect on CED. While as the axial compression ratio reached 0.26 and 0.33, compared with specimens having circular stirrups, the CED of specimens with rectangular stirrups were 21.76% and 26.57% larger, respectively.

### 4.2 Lateral Displacement Curves

Displacement transducers DH0–DH8 recorded the lateral displacements at the 600 mm, 1200 mm, 1600 mm, 2000 mm, 2560 mm height respectively from the bottom of the shear walls. As shown in Fig. 11, the measured lateral displacement curves obtained through DH0~DH8 at the drifts of 0.6%, 1.0%, 1.6%, 2.0%, 2.5% and 3.0% evidence the

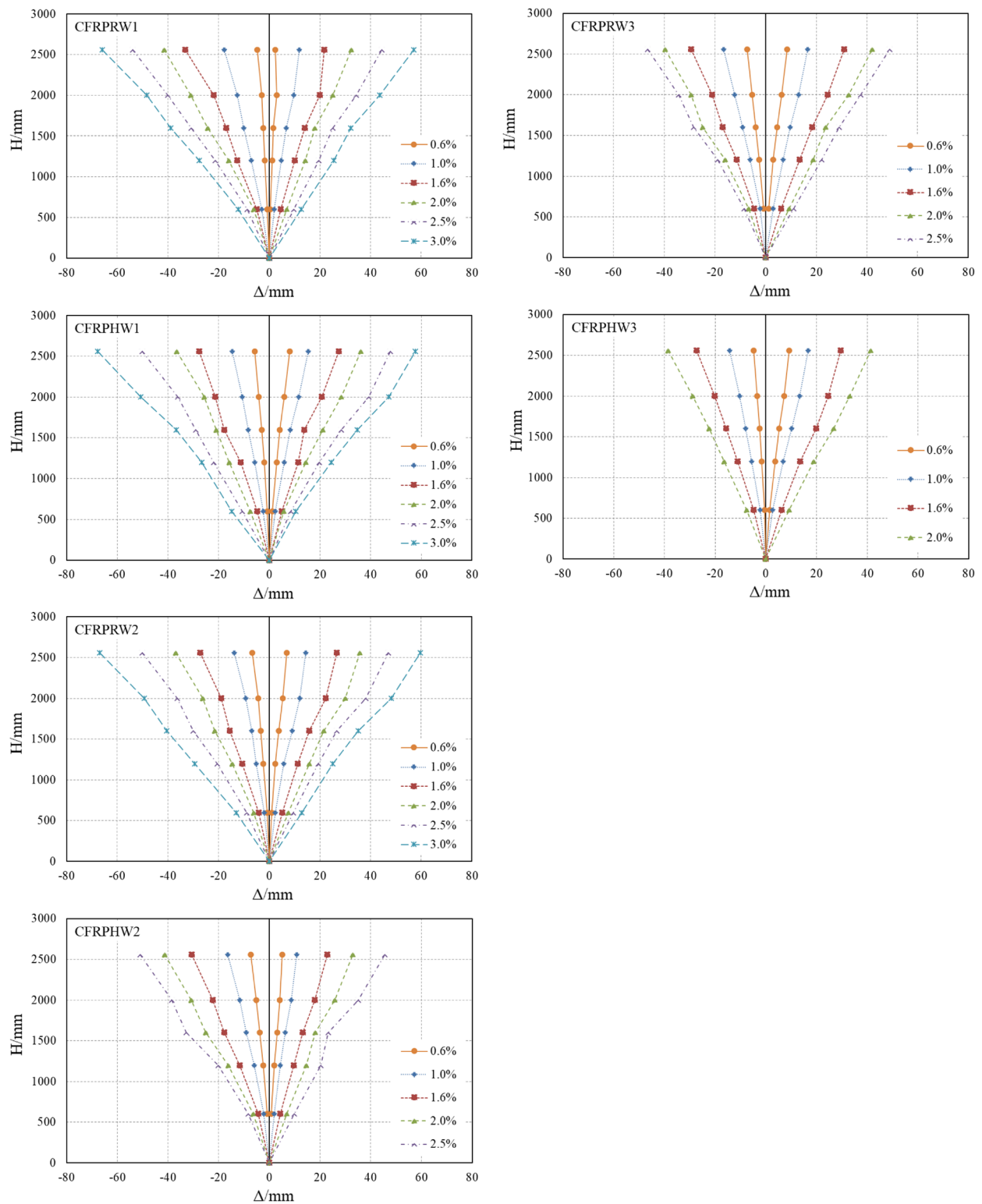




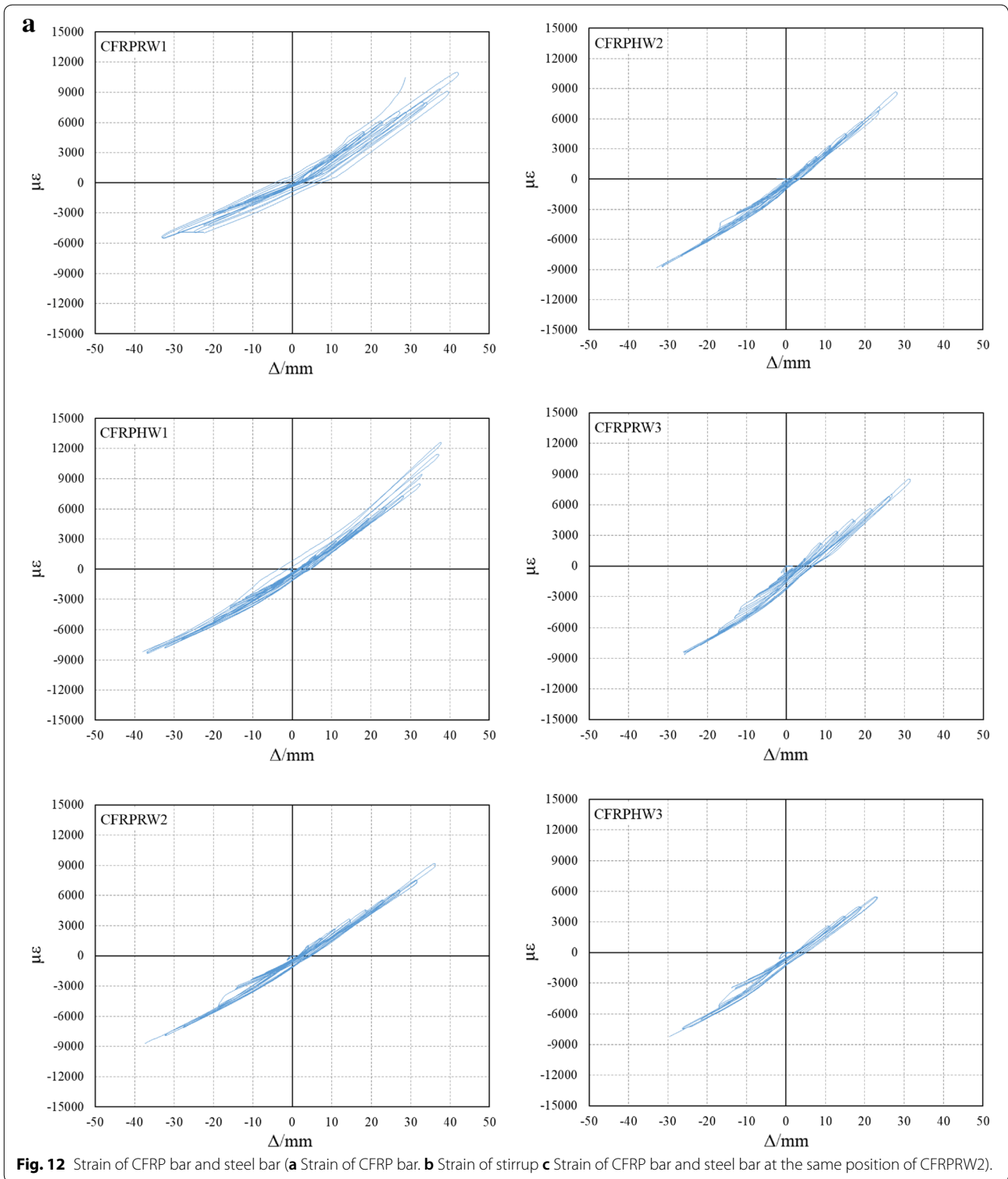
**Table 2** Cumulative Energy Dissipation (kN mm).

CFRPRW1	CFRPHW1	CFRPRW2	CFRPHW2	CFRPRW3	CFRPHW3
208568	214672	258328	212159	260627	205916

flexural mode exhibited during the test for all specimens. At the onset of loading, the lateral displacement increased linearly along the height, then as the loading continued, lateral displacement curves began to incline to the displacement



**Fig. 11** Lateral displacement curves.



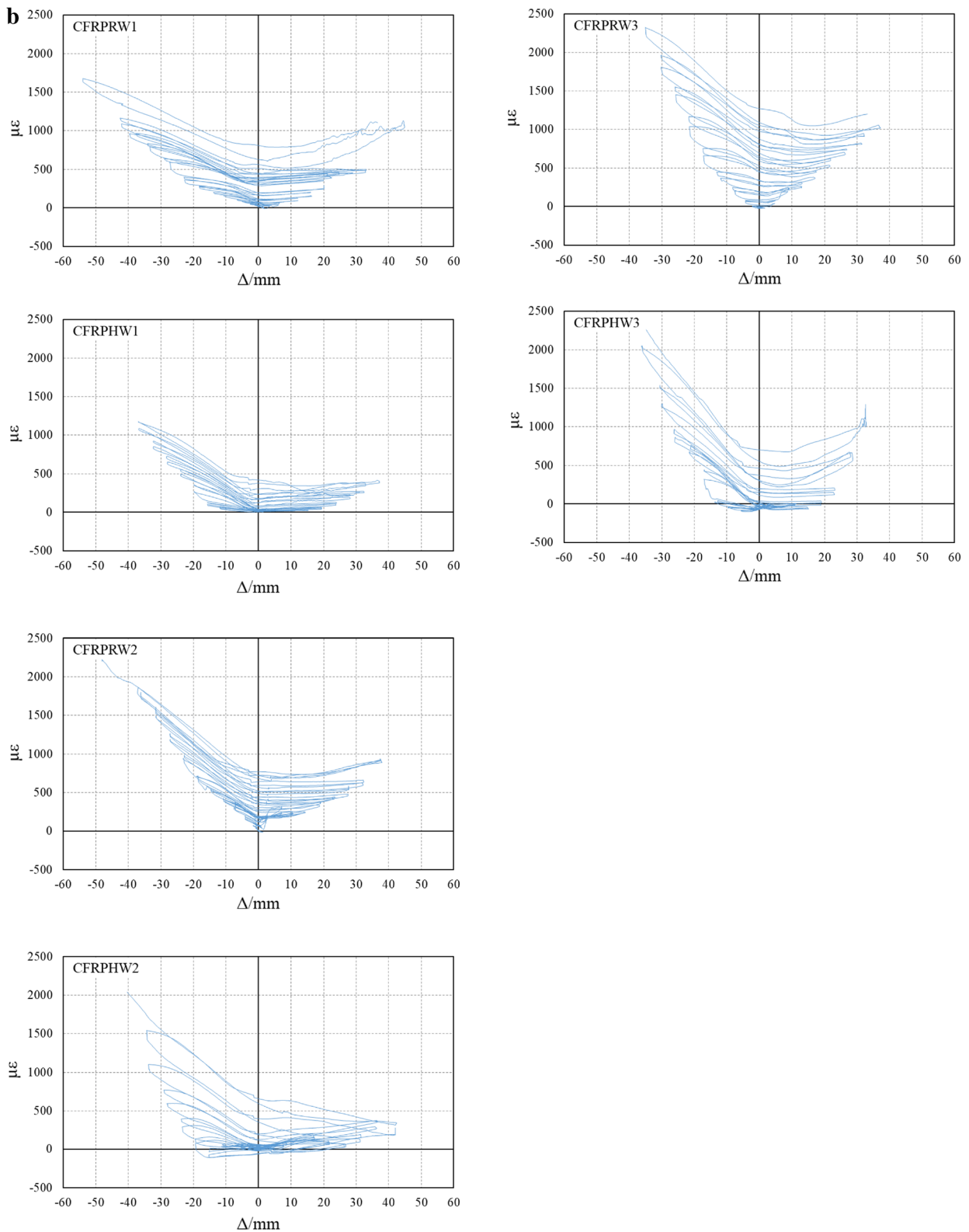


Fig. 12 (continued).

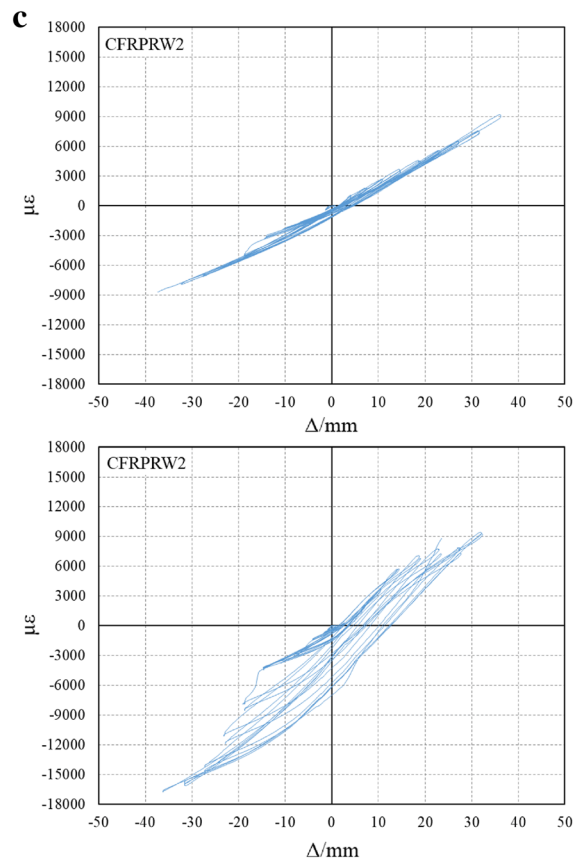


Fig. 12 (continued).

axis and the displacements of upper segments of specimens increased faster to present nonlinear variation along the height of wall due to the occurrence of plastic deformation.

#### 4.3 Strain Analysis of CFRP Bar and Steel Bar

Figure 12a displayed the strain–displacement curves of CFRP bars in the six shear walls. It could be concluded that the strains of CFRP bars varied cyclically with the drifts when shear walls were tested under the reversed cyclic lateral loading. And the strains represented the linear-varied trend at an angle of  $45^\circ$  taking the origin of coordinates as center roughly. When the drift reached 0, the strains of CFRP bars also almost recovered to 0, however, there were residual compression strains at the axial load ratio of 0.33. The phenomenon revealed that CFRP bars could present linear elasticity and offer resilience for shear walls to reduce residual deformations even at the large axial load ratio during the reversed cyclic lateral loading test. Besides, the resilience properties of CFRP bars were affected by the axial load ratio regardless of the forms of stirrups in boundary element.

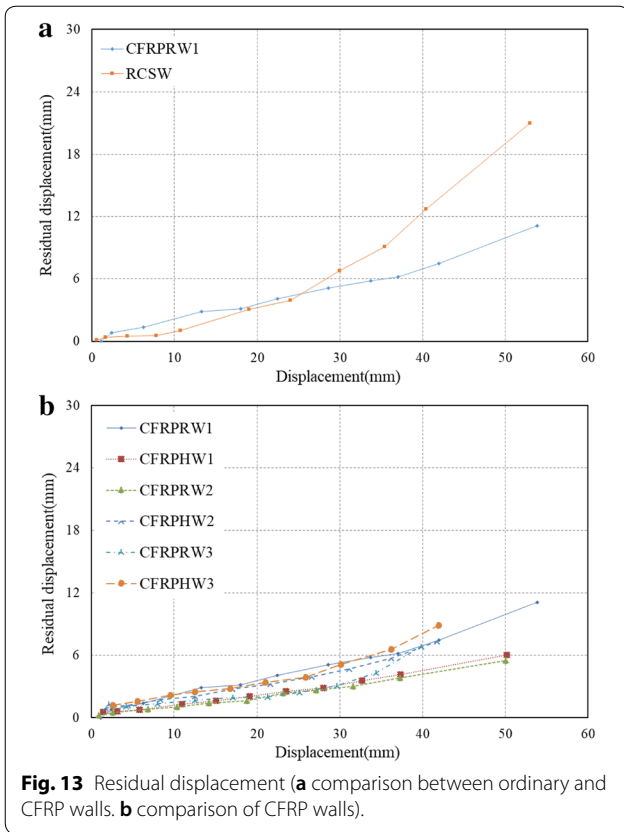
Figure 12b showed the strains of the stirrups in the boundary elements at the height of 100 mm from the

bottom of the shear walls. The strain of rectangular stirrup was quite higher than that of the circular stirrup at the same lateral displacement and axial load ratio, which meant that the performance and constraining function of the rectangular stirrup were much better. Furthermore, the strains of stirrups increased with the axial compression ratio and reached yielding at the axial compression ratios of 0.26 and 0.33.

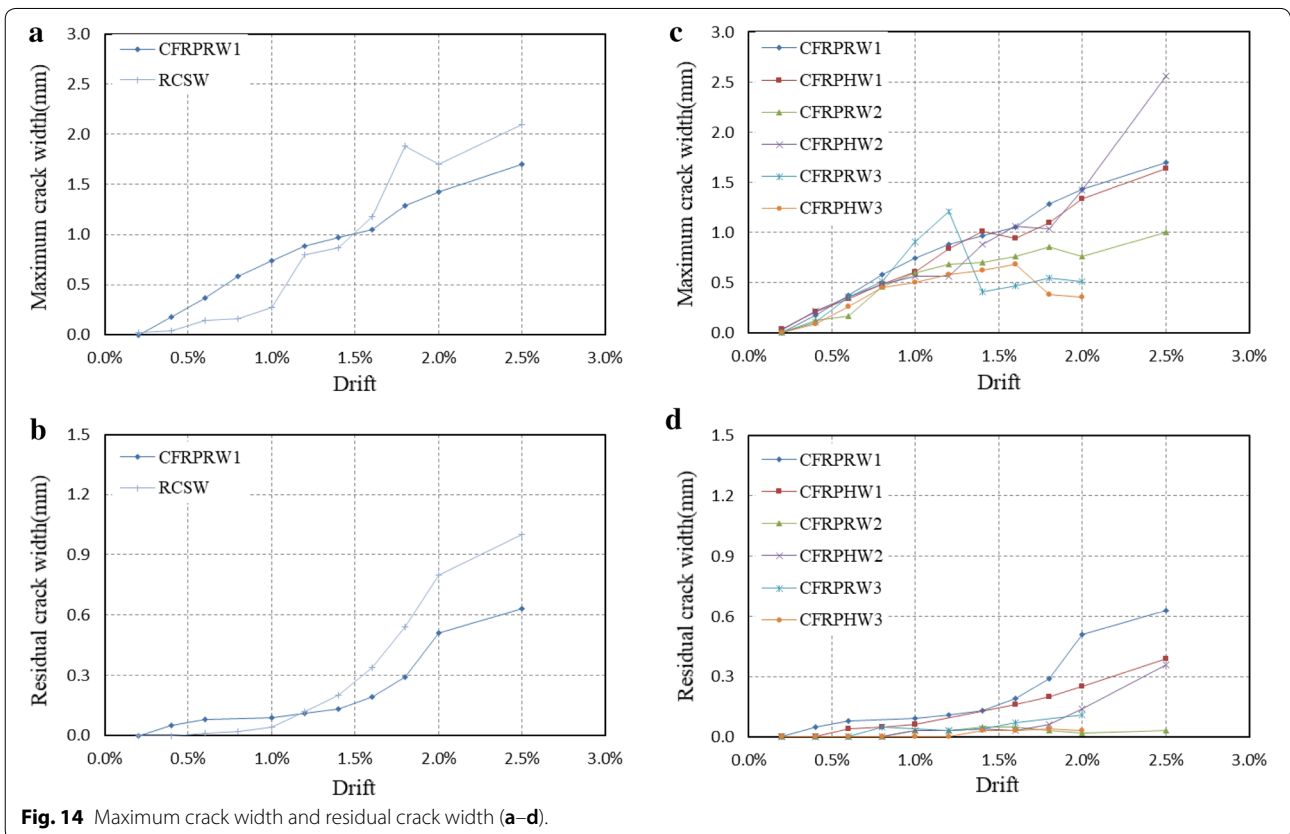
To compare the strains between CFRP bars and steel bars in the shear walls, Fig. 12c depicted the strains of CFRP and steel bars at the height of 100 mm from the bottom of the shear walls. The CFRP bars in the shear walls remained good linear elasticity under reversed cyclic load, though the steel bars yielded at the large drift resulting in obvious plastic deformation. The linear elasticity of CFRP bar could produce self-centering ability for the shear walls, while the plastic deformation of steel bars contributed to the energy dissipation.

#### 4.4 Residual Deformation and Residual Crack Width

Residual deformation and residual crack width were two important parameters to assess the resilient performance of shear wall specimens, both of which had great



influence on the reparability of shear walls after earthquake. Figure 13 presented the relative curves of peak and residual displacement after unloading at each drift level. The comparison of residual displacement–displacement relationship of walls using ordinary deformed steel bars and CFRP bars are shown in Fig. 13a. CFRPRW1 exhibited little residual displacement during the whole test. While the residual displacement of RCSW increased sharply to large value with the increase of the displacement. According to the result, Using CFRP bars can reduce the residual displacement from 20.97 mm to 11.10 mm after unloading from the displacement of 54 mm. The residual displacement–displacement curves of walls reinforced with CFRP bars are shown in Fig. 13b, at the incipient stage of loading, the residual displacement curves of the six specimens were similar and there was an upward trend for residual displacement with the increase of peak displacement. In subsequent stages of loading, the residual displacements were on rise, especially when the axial load ratio reached 0.33, the slope of residual displacement-peak displacement curve became steep obviously. The maximum residual displacement of CFRPRW1 was 11.10 mm and the corresponding peak displacement was 53.83 mm, which meant the deformation recovered 79.83% after unloading. The maximum



residual displacements of CFRPHW1, CFRPRW2, CFRPHW2, CFRPRW3 and CFRPHW3 were 6.03 mm, 5.51 mm, 7.31 mm, 6.83 mm and 8.86 mm, respectively. And the corresponding peak displacements were 50.21 mm, 50.07 mm, 41.73 mm, 39.85 mm and 41.92 mm. The deformations of those specimens recovered 87.99%, 89.00%, 82.48%, 82.86% and 78.66%, respectively. The conclusion could be drawn that placing CFRP bars as longitudinal tensile material could make the lateral deformation recover a lot after the reversed cyclic loading.

Figure 14 illustrated the variation curves with drift ratios of the maximum crack width and residual crack width after unloading. According to Fig. 14a, the maximum crack width of RCSW increased sharply with the drift and eventually reached to 2.1 mm which was 24% larger than CFRPRW1 at the drift ratio of 2.5%. Besides, the ordinary RC shear wall RCSW had residual crack width of 1.0 mm at 2.5% drift, while the residual crack width of CFRPRW1 was only 0.63 mm. Figure 14c, d present the crack widths of CFRPRW. In the beginning of loading, the variation tendency of maximum crack widths was similar for the six specimens, and the residual crack width was almost 0 within 0.6% drift. As the drift increased, the maximum crack widths increased inversely with the axial load ratio, while the slopes of residual crack width variation curves became steep for all specimens with the increasing axial load ratio. When the drift ratio was 2.5%, the maximum crack width of CFRPRW1 was 1.70 mm, and the corresponding residual crack width after unloading was 0.63 mm, which meant the crack width reduced by 62.94%. The other five specimens CFRPHW1, CFRPRW2, CFRPHW2, CFRPRW3, CFRPHW3 had the maximum crack widths of 1.64 mm, 1.00 mm, 2.56 mm, 0.59 mm and 0.36 mm, respectively. And their corresponding residual crack widths were 0.39 mm, 0.03 mm, 0.36 mm, 0.11 mm and 0.03 mm. It could be obtained that the crack widths reduced by 76.22%, 97.00%, 85.90%, 78.43% and 91.67% respectively after unloading. The conclusion could be drawn that the crack widths of all shear walls reduced a lot after the reversed cyclic loading.

The analysis above concluded that all CFRP bars reinforcing specimens had little deformation and crack width after unloading, which showed great resilience of deformation and crack.

#### 4.5 Stiffness Degradation

Figure 15 shows stiffness degradation curves of specimens. RCSW exhibits larger initial stiffness than CFRPRW1 until the displacement of 20 mm, after which RCSW and CFRPRW1 had almost similar stiffness degradation. The reason account for that phenomenon is

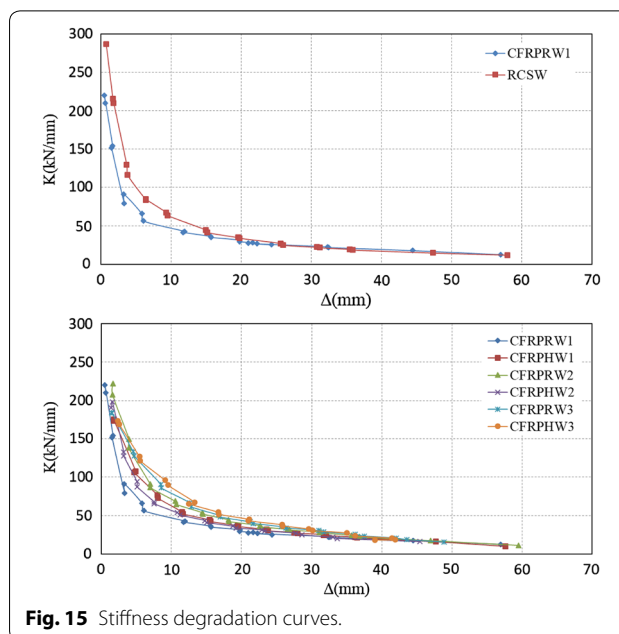


Fig. 15 Stiffness degradation curves.

that the Young’s modulus of steel bar is larger than that of CFRP bars, so ordinary RC shear wall had large initial stiffness. As for shear walls reinforced with CFRP bars, all specimens had similar stiffness degradation tendency. The stiffness degrades rapidly until the displacement of 6 mm. Then the stiffness degradation become tardy with the increase of displacement. The effects of axial load ratio on stiffness degradation can be concluded that stiffness degradation become slow as axial load ratio increases. Stirrup type also influences stiffness degradation. Shear walls with rectangular stirrups had rapid stiffness degradation than that with circular stirrups at the axial load ratios of 0.17 and 0.26. When the axial load ratio reached 0.33, there were no significant differences between these two stirrup types.

#### 5 Conclusions

RC shear walls reinforced with CFRP bars in boundary elements under reversed cyclic loading were researched experimentally. The following conclusions can be drawn.

1. Using CFRP bars in boundary elements can increase the peak lateral resistance by 20.1%, meanwhile reduce the residual displacement and crack width by 47.1% and 37.0%, respectively. Besides, CFRP bars can improve crack propagation and concrete spalling and provide stable resistance and resilience for shear walls.
2. The failures of shear walls reinforced with both CFRP bars and steel bars are in conformity with flexible-shear failure mode (mainly flexible failure) with fully

developed cracks. The concrete spalling area become larger with the increase of the axial load ratio. Different forms of stirrups in boundary elements have little effects on the concrete spalling area. However, there are a decline of the height of crack propagation on the wall panel and the extension of the spalling area at the bottom of the walls as increasing axial load ratio.

3. When the axial load ratio is relatively small, the peak loads of shear walls with rectangular stirrups are slightly larger than that of walls with circular stirrups, while the energy dissipation of the latter one is relatively better at the same drift. As the axial load ratio goes up, the results show an increase of the peak load of shear walls, as well as a decrease of the corresponding deformation and ultimate deformation. Besides, the stiffness degradation become slow. And at the axial load ratio of 0.33, the peak load, energy dissipation, stiffness degradation and ultimate displacement of shear walls are quite similar for both forms of stirrups.
4. The strains of rectangular stirrups are much higher than that of circular stirrups at the same axial load ratio. What is notable from the result is that the shear walls using rectangular stirrups present larger constraining force to the core concrete than circular stirrups to show larger strength and deformation capacity.
5. Satisfactory resilience of the six shear walls is obtained by using CFRP bars. The residual deformations of the shear walls recover to less than 25% of the corresponding peak deformations, and the minimum value is about 11%. The residual crack widths of the shear walls recover to less than 40% of the corresponding maximum crack widths, the minimum result is about 3%.

#### Acknowledgements

The authors acknowledge the Kobe University, Japan for the academic co-operation. The corresponding author would to acknowledge the China Scholarship Council and Zhengzhou University for supporting his overseas study scholarship.

#### Authors' contributions

JZ and FS planed the experiments, analyzed the data, and wrote the paper. FS and CS conducted the experiments and summed up the test data. YS and LY improved the experimental program and revised the paper. All authors read and approved the final manuscript.

#### Funding

Experimental work described in this paper was financially supported by the National Key R&D Program of China (2016YFE 0125600) and Program for Innovative Research Team of Education Ministry of China (IRT\_16R67).

#### Availability of data and materials

The data analyzed in the study are available from the corresponding author on reasonable request.

#### Competing interests

The authors declare that they have no competing interests.

#### Author details

<sup>1</sup> School of Mechanics and Safety Engineering, Zhengzhou University, Zhengzhou, Henan 450001, China. <sup>2</sup> School of Civil Engineering, Zhengzhou University, Zhengzhou, Henan 450001, China. <sup>3</sup> Graduate School of Engineering, Kobe University, Kobe, Hyogo 657-8501, Japan.

Received: 29 July 2019 Accepted: 15 November 2019

Published online: 10 January 2020

#### References

- Bi, L. (2013). Study of performance of eccentric compression column reinforced with hybrid FRP bars. Dissertation, Chongqing University (in Chinese).
- Brown, V. L., & Bartholomew, C. L. (1993). FRP reinforcing bars in reinforced concrete members. *ACI Materials Journal*, 90(1), 34–39.
- Cai, Z., Wang, D., & Wang, Z. (2017). Full-scale seismic testing of concrete building columns reinforced with both steel and CFRP bars. *Composite Structures*, 178, 195–209.
- Chen, J. (2015). Experimental study on the seismic behavior of CFRP-reinforced concrete shear wall. Dissertation, Zhengzhou University. (in Chinese).
- Chen, T., & Zheng, T. (2016). Review of earthquake damage losses in mainland China in 2015. *Journal of Catastrophology*, 31(3), 133–137. (in Chinese).
- Clubley, S. K., Moy, S. S. J., & Xiao, R. Y. (2003a). Shear strength of steel–concrete–steel composite panels. Part I—testing and numerical modelling. *Journal of Constructional Steel Research*, 59(6), 781–794.
- Clubley, S. K., Moy, S. S. J., & Xiao, R. Y. (2003b). Shear strength of steel–concrete–steel composite panels Part II—detailed numerical modelling of performance. *Journal of Constructional Steel Research*, 59(6), 795–808.
- Dang, X., Lu, X., & Zhou, Y. (2013). Study on seismic performance of a rocking wall with bottom horizontal slits. *Earthquake Engineering and Engineering Dynamics*, 33(5), 182–189. (in Chinese).
- Dang, X., Lu, X., & Zhou, Z. (2014). Experimental study and numerical simulation of self-centering shear walls with horizontal bottom slit. *Earthquake Engineering and Engineering Dynamics*, 34(4), 154–161. (in Chinese).
- Du, X., Wang, Z., & Zhan, J. (2012). Experimental studies on the seismic performance of concrete beams prestressed with FRP tendons. *China Civil Engineering Journal*, 45(2), 43–50. (in Chinese).
- El-Gamal, S., El-Salakawy, E., & Benmokrane, B. (2005). Behavior of concrete bridge deck slabs reinforced with fiber-reinforced polymer bars under concentrated loads. *ACI Structural Journal*, 102(5), 727–735.
- El-Mogy, M., El-Ragaby, A., & El-Salakawy, E. (2013). Experimental testing and finite element modeling on continuous concrete beams reinforced with fibre reinforced polymer bars and stirrups. *Canadian Journal of Civil Engineering*, 40(11), 1091–1102.
- Eom, T., Park, H., Lee, C., Kim, J., & Chang, I. (2009). Behavior of double skin composite wall subjected to in-plane cyclic loading. *Journal of Structural Engineering*, 135(10), 1239–1249.
- Gao, D., Zhao, G., & Brahim, B. (2001). Experimental study of flexural properties of FRP-reinforced concrete beam. *Industrial Construction*, 31(9), 41–44. (in Chinese).
- Ghazizadeh, S., & Cruz-Noguez, C. A. (2018). Damage-resistant reinforced concrete low-rise walls with hybrid GFRP-steel reinforcement and steel fibers. *Journal of Composites for Construction*, 22(2), 04018002.
- Gong, Y., Zhang, J., Jiang, L., & Tu, Y. (2010). Aseismic behavior of concrete columns reinforced with CFRP. *Journal of Central South University: Science and Technology*, 41(4), 1506–1513. (in Chinese).
- Hasaballa, M. H., El-Ragaby, A., & El-Salakawy, E. (2011). Seismic performance of exterior beam–column joints reinforced with glass fibre reinforced polymer bars and stirrups. *Canadian Journal of Civil Engineering*, 38(10), 1092–1102.
- Hitaka, T., & Matsui, C. (2003). Experimental study on steel shear wall with slits. *Journal of Structural Engineering*, 129(5), 586–595.
- Jiang, H., & Liu, Q. (2015). State-of-the-art of the research advances on resilient shear walls. *Journal of Vibration and Shock*, 34(7), 51–58. (in Chinese).

- Li, H., Xiao, S., & Huo, L. (2008). Damage investigation and analysis of engineering structures in the Wenchuan Earthquake. *Journal of Building Structures*, 29(4), 10–19. **(in Chinese)**.
- Lu, X., Quan, L., & Jiang, H. (2017). Research trend of earthquake resilient structures seen from 16WCEE. *Earthquake Engineering and Engineering Dynamics*, 37(3), 1–9. **(in Chinese)**.
- Lu, X., Zhou, Y., & Chen, C. (2014). Research progress on innovative earthquake-resilient structural systems. *Earthquake Engineering and Engineering Dynamics*, 1(4), 130–139. **(in Chinese)**.
- Ministry of Housing and Urban-Rural Development of the People's Republic of China. (2015). JGJ/T 101-2015 Specification for seismic test of buildings **(in Chinese)**.
- Mohamed, N. (2013). Strength and drift capacity of GFRP-reinforced concrete shear walls. Dissertation, University of Sherbrooke.
- Mohamed, N., Farghaly, A. S., Benmokrane, B., & Neale, K. W. (2014a). Flexure and shear deformation of GFRP-reinforced shear walls. *Journal of Composites for Construction*, 18(2), 04013044.
- Mohamed, N., Farghaly, A. S., Benmokrane, B., & Neale, K. W. (2014b). Experimental investigation of concrete shear walls reinforced with glass fiber-reinforced bars under lateral cyclic loading. *Journal of Composites for Construction*, 18(3), A4014001.
- Takahashi, Y., Takeda, T., Takemoto, Y., & Takagai, M. (1973). Experimental study on thin steel shear walls and particular bracing under alternating horizontal loading. *Proc., IABSE Symp., Resistance and Ultimate Deformability of Structures Acted on by Well Defined Repeated Loads*, Lisbon, Portugal, pp. 185–191.
- Tobbi, H., Farghaly, A. S., & Benmokrane, B. (2012). Concrete columns reinforced longitudinally and transversally with glass fiber-reinforced polymer bars. *ACI Structural Journal*, 109(4), 551–558.
- Tong, X. (2016). The study on seismic behavior and design method of reactive power concrete shear walls. Dissertation, Hunan University **(in Chinese)**.
- Tong, X., & Fang, Z. (2016). Study on seismic performance of super high-rise structure with reactive powder concrete. *Building Structure*, 46(03), 6–11. **(in Chinese)**.
- Tong, X., Fang, Z., & Luo, X. (2016). Experimental study on seismic behavior of reactive powder concrete shear walls. *Journal of Building Structures*, 37(01), 21–30. **(in Chinese)**.
- Tong, X., Hajjar, J. F., Schultz, A. E., & Shield, C. K. (2005). Cyclic behavior of steel frame structures with composite reinforced concrete infill walls and partially-restrained connections. *Journal of Constructional Steel Research*, 61(4), 531–552.
- Wu, H., Lu, X., Jiang, H., Shi, W., & Li, J. (2016). Experimental study on seismic performance of prestressed precast concrete shear walls. *Journal of Building Structures*, 37(5), 208–217. **(in Chinese)**.
- Yuan, W., Zhao, J., Sun, Y., & Zeng, L. (2018). Experimental study on seismic behavior of concrete walls reinforced by PC strands. *Engineering Structures*, 175, 577–590.
- Zeng, L. (2017). Study on seismic behaviors of shear walls by steel strands concrete. Dissertation, Zhengzhou University. **(in Chinese)**.
- Zhao, Q. (2016). The seismic behaviors of shear walls reinforced by CFRP bars and steel bars. Dissertation, Zhengzhou University. **(in Chinese)**.
- Zhao, J. (2019). Seismic and self-centering behavior of shear-walls reinforced with high strength bars. *Journal of Building Structures*, 40(3), 172–179. **(in Chinese)**.

### Publisher's Note

Springer Nature remains neutral with regard to jurisdictional claims in published maps and institutional affiliations.

Submit your manuscript to a SpringerOpen® journal and benefit from:

- Convenient online submission
- Rigorous peer review
- Open access: articles freely available online
- High visibility within the field
- Retaining the copyright to your article

---

Submit your next manuscript at ► [springeropen.com](https://www.springeropen.com)

---